Journal of
MATERIALS RESEARCH

Resonant Raman effect in single-wall carbon nanotubes

M. A. Pimenta,[a] A. Marucci, S. D. M. Brown, and M. J. Matthews
Department of Physics, Massachusetts Institute of Technology, Cambridge, Massachusetts 02139

A. M. Rao and P. C. Eklund
Department of Physics and Astronomy and Center for Applied Energy Research, University of Kentucky, Lexington, Kentucky 40506

R. E. Smalley
Department of Chemistry and Center for Nanoscale Technology & Science, Rice University, Houston, Texas 77005

G. Dresselhaus
Francis Bitter Magnet Laboratory, Massachusetts Institute of Technology, Cambridge, Massachusetts 02139

M. S. Dresselhaus
Department of Electrical Engineering and Computer Science and Department of Physics, Massachusetts Institute of Technology, Cambridge, Massachusetts 02139

(Received 3 March 1998; accepted 7 May 1998)

A resonant Raman study of single-wall carbon nanotubes (SWNT) using several laser lines between 0.94 and 3.05 eV is presented. A detailed lineshape analysis shows that the bands associated with the nanotube radial breathing mode are composed of a sum of individual peaks whose relative intensities depend strongly on the laser energy, in agreement with prior work. On the other hand, the shape of the Raman bands associated with the tangential C–C stretching motions in the 1500–1600 cm^{-1} range does not depend significantly on the laser energy for laser excitation energies in the ranges 0.94–1.59 eV and 2.41–3.05 eV. However, new C–C stretching modes are observed in the spectra collected using laser excitations with energies close to 1.9 eV. The new results are discussed in terms of the difference between the 1D electronic density of states for the semiconducting and metallic carbon nanotubes.

I. INTRODUCTION

Since the discovery of carbon nanotubes in the early 1990s,[1] theoretical work has shown that various physical properties should be strongly dependent on the nanotube diameter and chirality.[2–4] This dependence is ultimately related to the way that the two-dimensional Brillouin zone of the graphene sheet is folded into the one-dimensional Brillouin zone of the carbon nanotubes.[5] Due to the large length-to-diameter ratio for the nanotubes, the electron motion is normally confined to the tube axis, and therefore, for small diameter nanotubes, the one-dimensional (1D) density of electronic states exhibits sharp singularities below and above the Fermi level E_F as shown in Fig. 1. The carbon nanotube can be metallic or semiconducting, depending on the magnitude and direction of its chiral vector. As shown in Fig. 1, the structures of the electronic density of states (DOS) for semiconducting and metallic nanotubes are significantly different. Within each category, there are singularities in the 1D density of states, and the separation between the singularities increases with decreasing tube diameter. Furthermore, the phonon spectrum of the nanotubes, which is associated with the folding of the phonon dispersion curves for a single graphene sheet, is also dependent on the tube diameter and chirality.[7]

The experimental verification of these predictions was recently facilitated by the development of a method for the synthesis and purification of bundles of single-wall carbon nanotubes.[8,9] Raman spectroscopy is one of the techniques that has strongly contributed to the understanding of the one-dimensional properties of carbon nanotubes, since it can probe both the phonon spectrum and the electronic structure through the resonant Raman effect.[10] A recent Raman investigation of single-wall carbon nanotubes (SWNT's)[11] confirmed earlier theoretical predictions concerning the one-dimensional character of the electronic structure and the density of states. The most striking result reported in this work[11] was the dependence of the position and shape of specific Raman bands on the exciting laser energy, and this effect was explained in terms of a diameter-selective Raman

[a]Permanent address: Departamento de Fisica, Universidade Federal de Minas Gerais, Belo Horizonte, 30123-970 Brazil. e-mail: mpimenta@fisica.ufmg.br

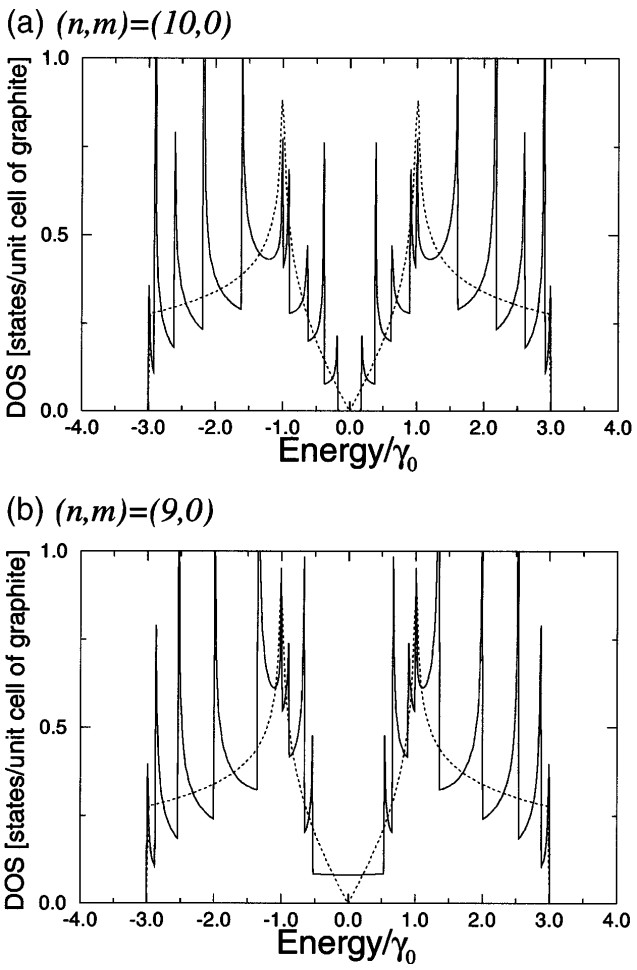

FIG. 1. Electronic 1D density of states per unit cell of a 2D graphene sheet for two $(n,0)$ zigzag nanotubes: (a) The (10,0) nanotube which has semiconducting behavior, and (b) the (9,0) nanotube which has metallic behavior. Also shown in the figure is the density of states for a 2D graphene sheet (dotted curve).[6]

scattering process, which can be understood by referring to Fig. 2 which shows the frequency dependence of the various Raman-allowed modes for armchair nanotubes as a function of nanotube diameter.

This diameter-selective Raman scattering[11] is particularly important for the Raman band at about 180 cm^{-1}, which is associated with the radial breathing mode (RBM) of the carbon nanotube. According to theoretical predictions,[2,3,12] the frequency of the RBM is inversely proportional to the tube diameter and independent of chirality. In a sample containing tubes with a distribution of different diameters, the RBM Raman band around 180 cm^{-1} is, in fact, composed of a superposition of single peaks associated with individual nanotubes. The intensity of each one of these peaks is enhanced when the photon energy of the excitation laser is in resonance with an allowed optical transition between singularities in the 1D density of electronic states.[13] Since the energy difference between singularities in the valence and conduction

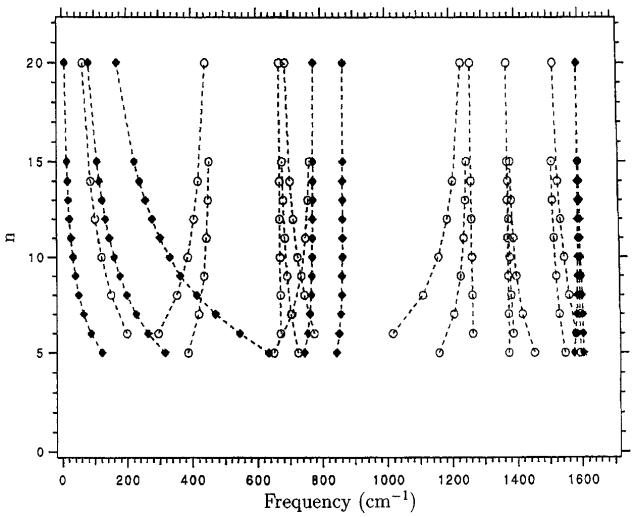

FIG. 2. The armchair index n versus mode frequency for the Raman-active modes of single-wall armchair (n,n) carbon nanotubes.[11] For armchair nanotubes, the diameter is given by $d_t = 1.38 \times n$ Å.

bands depends on the nanotube diameter and chirality, each laser line preferentially probes specific nanotubes. Therefore, the frequency and the shape of the RBM band in a multicomponent sample change when the sample is probed with different laser lines.

In this work we will focus on the analysis of the high frequency Raman band associated with the C–C stretching modes in the range 1500–1600 cm^{-1}, obtained with a number of different laser excitation frequencies between 0.94 eV and 3.05 eV. Experimental results are compared with the resonant behavior of the radial breathing mode and are related to the theoretical predictions that have been made for the phonon spectrum and the electronic density of states for the carbon nanotubes. Specifically, we find the appearance of new high-frequency modes in the spectra obtained with laser energies $E_{laser} \approx 1.9$ eV, which were not present in the spectra obtained with higher and lower laser energies. These modes are ascribed to metallic nanotubes, and their enhancements are due to the resonance of the incident photon with the lowest energy electronic transition for the metallic nanotubes, which occurs at approximately 1.9 eV in the case of the SWNT's present in our sample. This result gives, for the first time, experimental evidence for differences between the phonon spectra for metallic and semiconducting nanotubes and the influence of the conduction electrons on the phonon frequencies of the metallic tubes.

II. EXPERIMENTAL DETAILS

The SWNT's have been synthesized by the laser vaporization of a carbon target containing 1 to 2 atom % of Ni/Co in a furnace at 1200 °C.[8,11] The resultant material is composed of a mat of carbon ropes, and a typical rope

is seen in the transmission electron microscope (TEM) as a bundle of SWNT's 10 to 20 nm in diameter and 10 to 100 μm in length.[11] The nanotube diameter distribution obtained from the TEM contrast image for our sample exhibits a peak at about 1.24 nm, and is very close to the diameter of the armchair (9,9) nanotube. The width of the distribution is consistent with the range of diameters between 1.0 and 1.6 nm. However, the mean diameter was also determined by x-ray diffraction and was near that of a (10,10) nanotube.[8,11] Recent results suggest that the tube diameter distribution is sensitive to the oven temperature used in the synthesis.[12]

Raman scattering experiments were performed at ambient conditions using a backscattering geometry for the following laser excitation lines: krypton 647.1 nm and 406.7 nm (1.92 eV and 3.05 eV); argon 514.5 nm, 488 nm, and 457.9 nm (2.41 eV, 2.54 eV, and 2.71 eV, respectively); He–Ne 632.8 nm (1.96 eV); Nd:YAG 1320 nm and 1064 nm (0.94 eV and 1.17 eV); and an AlGaAs diode 780 nm (1.59 eV). The spectral resolution of the Raman systems was better than 2 cm^{-1}.

III. SYMMETRY ANALYSIS

The symmetry of a carbon nanotube is given by its chiral vector $n\mathbf{a_1} + m\mathbf{a_2}$, or (n, m), where $\mathbf{a_1}$ and $\mathbf{a_2}$ are the unit vectors in the two-dimensional (2D) hexagonal honeycomb lattice of a graphene sheet, and n and m are integers.[2,5] Three types of nanotubes are possible, depending on the value of (n, m): the armchair nanotubes where $n = m$, zig-zag nanotubes where $m = 0$, and chiral nanotubes where $n \neq m \neq 0$. A nanotube is metallic when $n - m$ is divisible by 3; otherwise it is semiconducting. All armchair nanotubes are metallic, while the zig-zag and chiral nanotubes can be metallic or semiconducting. The armchair and zig-zag nanotubes belong to the centro-symmetric D_{nh} and D_{nd} groups, depending on whether n is even or odd, respectively. The chiral nanotubes belong to the C_N nonsymmorphic group.

The diameter of the nanotube is related to the (n, m) values by[5]

$$d = a\sqrt{n^2 + m^2 + nm}/\pi\,, \qquad (1)$$

where the lattice constant on a graphene sheet a is taken to be 2.46 Å on a flat graphite sheet and 2.49 Å on a rolled-up nanotube cylinder.[2] The number of carbon atoms in the 1D unit cell (2N) depends on the tube diameter and on the chiral angle θ, which is also determined by the values of n and m.[5] However, the number of Raman-active modes does not depend on the tube diameter, but only on the type of nanotube. According to Table I, 16 Raman-active modes are expected for all armchair (n, n) nanotubes when n is even, and 15 Raman-active modes are expected for all the other nanotube types.[2,5]

In the present work, we discuss the laser excitation frequency dependence of the radial breathing mode (RBM) near 180 cm^{-1} and the Raman-active modes between 1500 and 1600 cm^{-1} associated with the tangential displacement C–C bond stretching motions of the nanotube (see Fig. 2). The radial breathing mode belongs to the identity representation (A_{1g} or A_1) and, according to theoretical predictions, its frequency is inversely proportional to the tube diameter, without any chirality dependence.[2,3] Theoretical calculations show that the high frequency Raman-active modes associated with the tangential C–C bond stretching motions have A_{1g}, E_{1g}, and E_{2g} (armchair and zigzag) [or A_1, E_1, and E_2 (chiral)] symmetries. The frequencies and number of Raman-active modes between 1500 and 1600 cm^{-1} depend on the diameter and chirality of the nanotube, and for the case of armchair (n, n) nanotubes, on whether n is even or odd. Therefore, several different modes are expected in a sample containing nanotubes of different types. However, within each type of nanotube, the three highest frequency modes between 1560 and 1600 cm^{-1} are expected to be very weakly dependent on the diameter of the nanotube, by perhaps an order of magnitude less than for the case of the diameter dependence of the radial breathing mode. In addition, the tangential modes near 1530 cm^{-1} with E_{1g} or E_{2g} (E_1 or E_2) symmetry are expected to show a diameter dependence of their mode frequencies that is intermediate between that for the modes near 180 cm^{-1} and in the range 1560–1600 cm^{-1}, as can, for example, be seen in Fig. 2 which shows the calculated diameter dependence of the Raman-active modes for armchair nanotubes.[2,4] The same kind of diameter dependence of the Raman-active RBM and the modes in the 1500–1600 cm^{-1} range occurs for zigzag and chiral nanotubes.[5]

TABLE I. Number and symmetries of Raman-active modes for different types of carbon nanotubes.

Nanotube structure	Point group	Raman-active modes	IR-active modes
Armchair (n, n) n even	D_{nh}	$4A_{1g} + 4E_{1g} + 8E_{2g}$	$A_{2u} + 7E_{1u}$
Armchair (n, n) n odd	D_{nd}	$3A_{1g} + 6E_{1g} + 6E_{2g}$	$2A_{2u} + 5E_{1u}$
Zigzag $(n, 0)$ n even	D_{nh}	$3A_{1g} + 6E_{1g} + 6E_{2g}$	$2A_{2u} + 5E_{1u}$
Zigzag $(n, 0)$ n odd	D_{nd}	$3A_{1g} + 6E_{1g} + 6E_{2g}$	$2A_{2u} + 5E_{1u}$
Chiral (n, m) $n \neq m \neq 0$	C_N	$4A + 5E_1 + 6E_2$	$4A + 5E_1$

IV. RESULTS

Figure 3 shows the high frequency Raman band associated with the tangential C–C stretching modes of the SWNT's, obtained with different laser lines from $0.94 \leqslant E_{\text{laser}} \leqslant 3.05$ eV. Note that the spectra obtained for E_{laser} in the ranges 0.94–1.59 eV and 2.41–3.05 eV are quite similar, whereas the spectrum obtained with $E_{\text{laser}} = 1.92$ eV is completely different, as previously reported by Rao *et al.*[11]

Let us first discuss these high frequency Raman bands obtained with the laser excitation in the ranges 0.94–1.59 eV and 2.41–3.05 eV. We note that these spectra are not sensitive to the laser excitation energy E_{laser}. Figure 4 shows the fitting of one of these typical bands ($E_{\text{laser}} = 2.41$ eV) by a sum of Lorentzian lines. At least six different peaks are necessary to give a good fit to the experimental data, and their frequencies are 1522, 1547, 1563, 1570, 1591, and 1600 cm^{-1}. All the other high frequency Raman bands obtained in the laser energy ranges 0.94–1.59 eV and 2.41–3.05 eV are similar and have been fitted using the same set of frequencies (with small variations of ± 2 cm^{-1}). The fitting parameters obtained from the analysis are given in Table II. We tentatively identify Raman lines #6, 7, and 9 which have relatively small linewidths with the calculated modes between 1560 and 1600 cm^{-1}, which theory predicts to have very little dependence on nanotube diameter as shown in Fig. 2 for the arm-chair nanotubes. The broader lines at 1522 cm^{-1} and 1547 cm^{-1} are identified with modes which are expected to exhibit an intermediate diameter dependence in their mode frequencies, as shown in Fig. 2. We do not at present have a clear explanation for the larger linewidth of Raman line #10 at 1600 cm^{-1}, which may be due to a superposition of unresolved Raman lines.

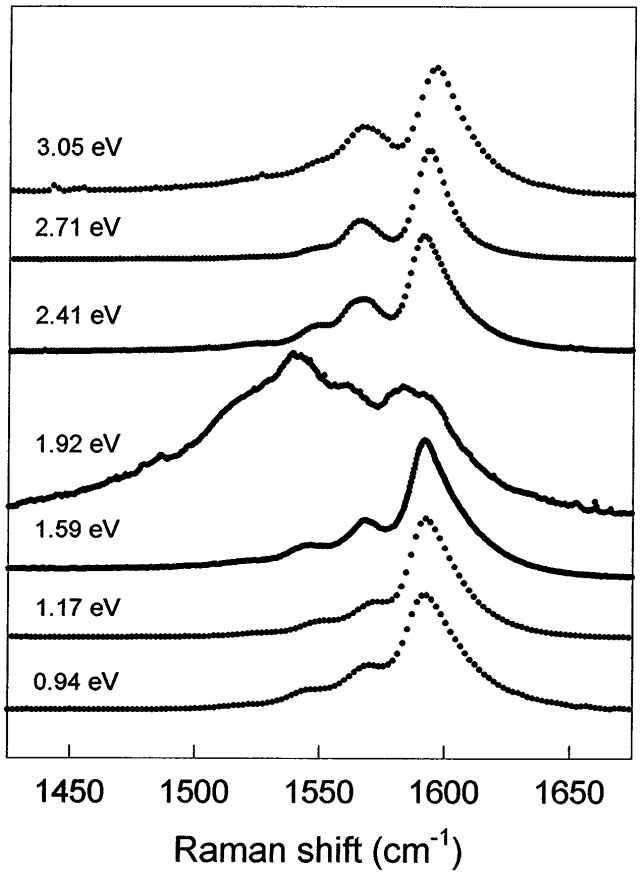

FIG. 3. Raman spectra of the tangential C–C stretching modes of single-wall carbon nanotubes obtained with different laser lines.

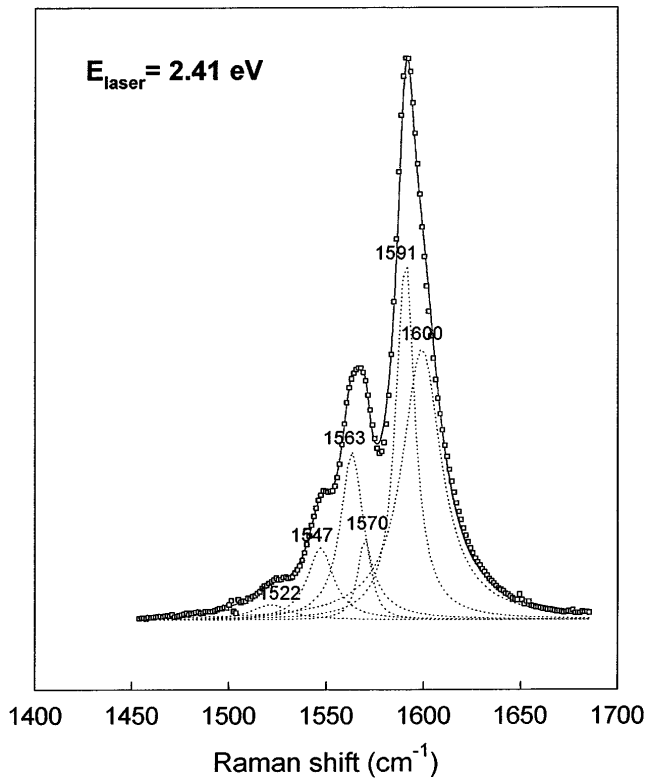

FIG. 4. Raman band associated with the C–C stretching modes of single-wall carbon nanotubes obtained using the laser excitation energy 2.41 eV. The dotted curves represent the individual Lorentzian components, and the solid curve represents the fit to the experimental data. The values of the fitting parameters are given in Table II.

Figure 3 shows that the high frequency Raman band obtained with the 1.92 eV laser excitation is completely different from all the other spectra. The spectrum obtained with laser excitation at 1.96 eV, and not shown in Fig. 3, is very similar to that obtained with $E_{\text{laser}} = 1.92$ eV. It is clear that new components appear in the spectrum using the 1.92 eV laser excitation. The anomalously shaped Raman band in Fig. 3 has also been fitted by means of a sum of Lorentzian peaks and the procedure adopted was the following. First, we found that the six lines used to fit the Raman spectra for the 0.94–1.59 eV and 2.41–3.05 eV laser excitation energies were also present in the 1.92 eV laser excitation

TABLE II. Frequencies (ω) and full-width at half-maximum intensity (γ) of the Lorentzian curves used to fit the bands associated with the C–C stretching modes of carbon nanotubes, obtained with different laser excitation energies. The units are in cm^{-1}.

Laser excitation	0.94 eV		1.17 eV		1.59 eV		1.92 eV		1.96 eV		2.41 eV		2.54 eV		2.71 eV		3.05 eV	
	ω	γ	ω	γ	ω	γ	ω	γ	ω	γ	ω	γ	ω	γ	ω	γ	ω	γ
Line #1	...	...	...	...	...	...	1515	42	1513	32	...	...	...	...	...	...	...	...
Line #2	1522	24	1523	24	1519	24	1522	24	1522	24	1522	24	1522	16	1522	24	1522	24
Line #3	...	...	...	...	...	...	1540	32	1537	30	...	...	...	...	...	...	...	...
Line #4	1547	23	1549	18	1545	24	1547	16	1549	15	1547	16	1549	16	1548	16	1546	20
Line #5	...	...	...	...	...	...	1558	20	1558	14	...	...	...	...	...	...	...	...
Line #6	1564	12	1563	14	1564	12	1563	14	1563	12	1563	14	1563	12	1564	12	1564	14
Line #7	1570	10	1570	11	1570	8	1570	9	1570	8	1570	8	1571	8	1570	8	1571	8
Line #8	...	...	...	...	...	...	1581	17	1581	18	...	...	...	...	...	...	...	...
Line #9	1591	18	1592	15	1592	15	1591	13	1593	12	1591	12	1593	12	1593	11	1594	12
Line #10	1603	33	1600	28	1603	30	1600	25	1601	26	1600	24	1601	26	1599	19	1600	22

spectrum. Therefore, we kept this set of six Lorentzian peaks using an average of the frequencies, linewidths and relative intensities for these six components from Table II. We then introduced the minimum number of new Lorentzian peaks necessary to fit the high frequency Raman band for the 1.92 eV laser excitation spectrum. Figure 5 shows the result for the best fit that was obtained. The dot-dashed curve in Fig. 5 represents the set of six peaks used to fit the bands obtained in the ranges 0.94–1.59 eV and 2.41–3.05 eV (see Fig. 4), the dotted curves represent the four new Lorentzian peaks, and the solid curve is the sum of all the Lorentzians needed to fit the experimental data. The values of the Lorentzian parameters (frequencies and FWHM's) used in the fitting are given in Table II. The frequencies of these four extra peaks are 1515, 1540, 1558, and 1581 cm^{-1}. We believe that it is significant that each of the new peaks shows about the same downshift in frequency with respect to a peak found in the spectra at all other laser frequencies. Thus the new peaks at 1515, 1540, 1558, and 1581 cm^{-1} are, respectively, identified with peaks in the dot-dashed curve at 1522, 1547, 1563, and 1591 cm^{-1}. We return to the discussion of these frequency shifts and their relative intensities in Sec. V.

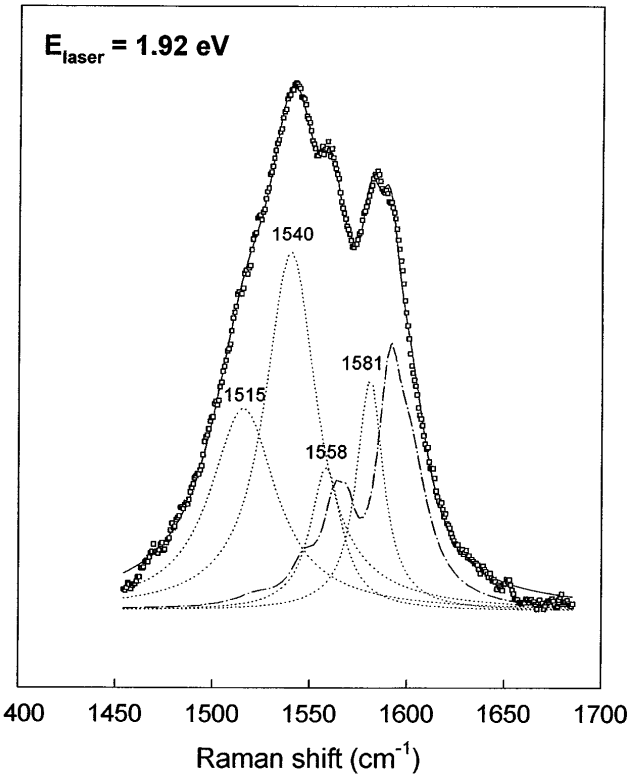

FIG. 5. Raman band associated with the C–C stretching modes of single-wall carbon nanotubes obtained using the laser excitation energy 1.92 eV. The dot-dashed curve represents the set of six peaks used to fit the bands obtained using laser excitation energies in the ranges 0.94–1.59 eV and 2.41–3.05 eV (see Fig. 3), the dotted curves represent the four new Lorentzian peaks, and the solid curve is the fitting of the experimental data. The values of the fitting parameters are given in Table II.

Figure 6 shows the Raman band associated with the radial breathing mode (RBM) of the SWNT's obtained with different laser lines, ranging from 1.17 to 2.71 eV in energy. Note that, in contrast to the case of the high frequency modes, the band shapes are completely different from one laser line to another, as first pointed out by Rao *et al.*[11] This result is consistent with the fact that the sample contains carbon nanotubes with different diameters and that the frequency of the RBM depends strongly on the nanotube diameter. The shape of the RBM band depends on the relative populations of each nanotube type that is in resonance at the particular excitation frequency. All the observed RBM bands have been fitted by means of a sum of Lorentzian peaks, as shown by the dotted lines in Fig. 6. Obviously, there are different sets of parameters that can fit the Raman bands equally well. We therefore adopted some restrictions on the fitting procedure in order to find the best set of parameters that is

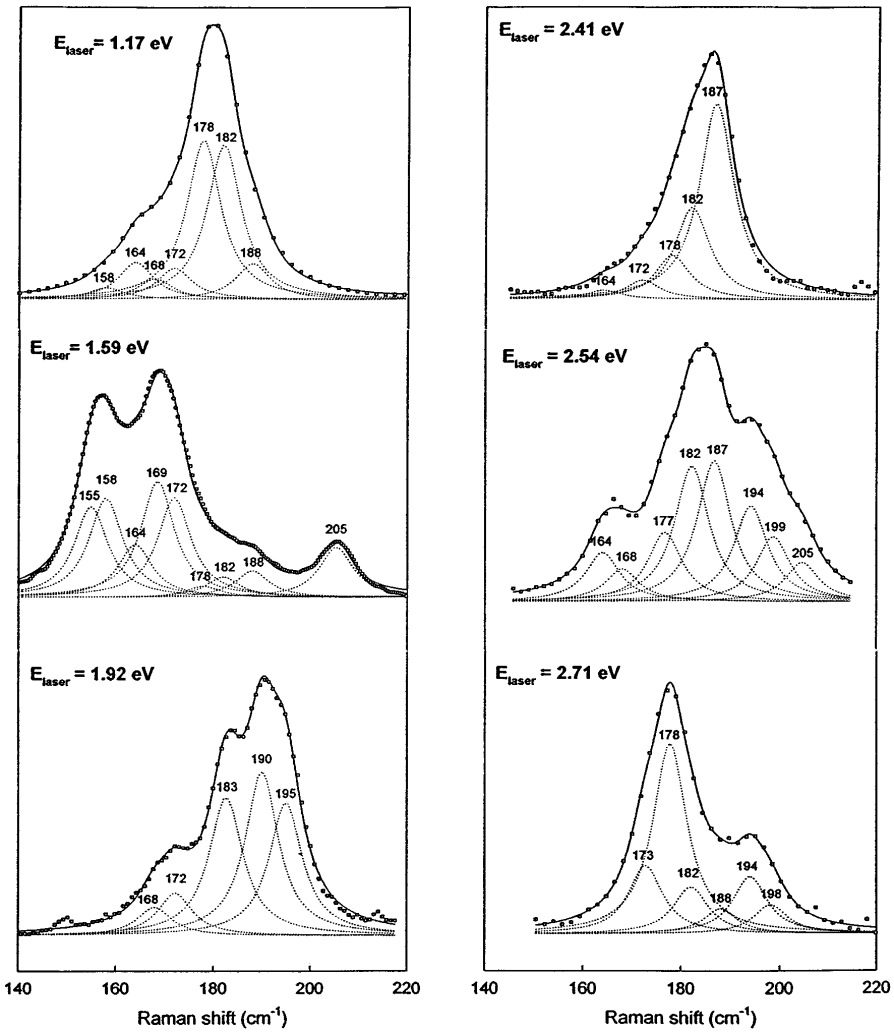

FIG. 6. Raman spectra of the radial breathing mode (RBM) of single-wall carbon nanotubes collected with six different laser lines: $E_{\text{laser}} = 1.17$ eV, 1.59 eV, 1.92 eV, 2.41 eV, 2.54 eV, and 2.71 eV. The dotted curves represent the individual Lorentzian curves and the solid curve represents the fit to the experimental data. All Lorentzian curves have the same linewidth, that is, FWHM = 8.4 cm^{-1}.

compatible with the theoretical principles and also with experimental results obtained from other techniques. All Lorentzian components were given the same width ($\sim$8.4 cm^{-1}) since the damping constant for the RBM is not expected to be strongly dependent on the nanotube diameter d for 1.0 nm $\leqslant d \leqslant$ 1.6 nm. The second constraint in the fitting process was to find the minimum number of phonon frequencies that fitted all the different Raman bands equally well. The frequencies of most of these individual peaks were obtained directly from inspection of the maxima in each Raman band. All six RBM Raman bands shown in Fig. 6 were then fitted by fixing the positions of the individual peaks, all of which were given the same width. Table III shows the frequencies of the peaks used to fit the six different Raman spectra shown in Fig. 6. Note that these values can be grouped in a set of 12 different frequencies (with small variations of ± 1 cm^{-1}). The full-width at half-maximum (FWHM) of the Lorentzians was taken to be 8.4 cm^{-1}, which is a typical value for the width of phonons in crystals (where we note that the sample is a bundle of SWNT's arranged in a two-dimensional triangular lattice).

According to theoretical predictions,[2,3,13] the value of the frequency of the RBM for SWNT's is inversely proportional to the nanotube diameter and independent of chirality. Bandow *et al.*[12] calculated the RBM frequencies for all types of SWNT's, and found that all frequencies fall on the straight line $\omega(d) = 223.75/d$, where ω is in units of cm^{-1} and d is in units of nm. Considering that the observed peaks occur in the range (155–205 cm^{-1}), the application of the above expression shows that the observed tubes have their diameters in the range (1.09–1.44 nm) and that the center of the distribution of the observed frequencies corresponds to a mean diameter around 1.25 nm. These values are

TABLE III. Frequencies (in cm^{-1}) of the Lorentzian curves used to fit the bands associated with the radial breathing mode (RBM) of carbon nanotubes, obtained with different laser excitation energies.[a]

Laser excitation	1.17 eV	1.59 eV	1.92 eV	2.41 eV	2.54 eV	2.71 eV
Line #1	···	155	···	···	···	···
Line #2	158	158	···	···	···	···
Line #3	164	164	···	164	164	···
Line #4	168	169	168	···	168	···
Line #5	172	172	172	172	···	173
Line #6	178	178	···	178	177	178
Line #7	182	182	183	182	182	182
Line #8	188	188	···	187	187	188
Line #9	···	···	190	···	···	···
Line #10	···	···	195	···	194	194
Line #11	···	···	···	···	199	198
Line #12	···	205	···	···	205	···

[a]The RBM bands obtained with the 0.94 eV and 3.05 eV laser lines were not analyzed because the signal was very faint and noisy.

compatible with the TEM results[11] on this sample, which show a range of diameters between 1.0 and 1.6 nm, and the mean diameter for this sample is consistent with the (9,9) nanotube.

V. DISCUSSION

We first focus our discussion on the resonant behavior of the high frequency modes in the range 1500–1600 cm^{-1}. Figure 3 shows that, with the exception of the band obtained with laser excitation at 1.92 eV, the Raman spectra obtained with several different laser lines are quite similar. This kind of behavior is consistent with theoretical predictions concerning the weak dependence of the tangential C–C stretching mode frequencies between 1560 and 1600 cm^{-1} on the nanotube diameter.[2,5] We note that the Raman spectra for all laser lines are dominated by the modes near 1590 cm^{-1}. The mode frequencies near 1540 cm^{-1}, which according to Fig. 2 show more diameter dependence, are typically very weak except for the spectrum for $E_{\text{laser}} = 1.92$ eV. The interesting result is the important change in the Raman intensity of the modes near 1540 cm^{-1} as the laser excitation energy approaches 1.9 eV.

Although the origin of these new extra Raman peaks is not yet well understood, we present here a proposed explanation which accounts for most of our observations. We argue that these new peaks may be attributed to a particular type of carbon nanotube, for which the Raman spectrum is enhanced only by using exciting laser energies close to 1.9 eV. It is well known that the electronic density of states (DOS) for the semiconducting SWNT's has a larger number of singularities within 1.5 eV of the Fermi level than for the metallic nanotubes.[5] This is illustrated in Fig. 1 for the case of zigzag nanotubes. According to recent calculations,[2,14,15] it is shown that within about ± 1.2 eV of the Fermi level, the 1D density of states curves for armchair, zigzag, and chiral *metallic* nanotubes with approximately the same diameter are similar, with the smallest energy separations ($E_{c1} - E_{v1}$) between $E^{-1/2}$ DOS singularities above and below the Fermi level for metallic nanotubes between 1.1 and 1.6 nm occurring for energies between 2.3 and 1.6 eV, respectively.[14] These calculations further show that the separations between the second pair of singularities ($E_{c2} - E_{v2}$) are greater than 3 eV for these SWNT's, where *v* and *c* refer to the valence and conduction bands. Likewise for *semiconducting* zigzag and chiral nanotubes of similar diameter, the 1D density of states curves are similar to each other but different from those for the metallic nanotubes (see Fig. 1). The calculations show that semiconducting SWNT's with diameters between 1.1 and 1.6 nm have an energy gap $\leqslant 1$ eV, and at least three singularities occur in the 1D density of states in the valence and conduction bands, whose energy separations $E_{ci} - E_{vj}$ are smaller than 3 eV, so that several different optical transitions with energies smaller than 3 eV are possible for each of the semiconducting SWNT's. Here the subscripts *i* and *j* refer to the order of the singularities relative to the Fermi level E_F, so that ($E_{c1} - E_{v1}$) corresponds to the lowest optical transition energy.

The theoretical predictions about the peaks in the electronic DOS have been recently confirmed by scanning tunneling spectroscopy (STS) experiments in SWNT's.[16] Wildöer *et al.* showed that the semiconducting SWNTs with diameters in the range 1.2–1.4 nm exhibit electronic gaps around 0.5–0.65 eV, whereas the metallic SWNTs exhibit larger "gaps" of ~1.7–2.0 eV corresponding to the energy separation ($E_{c1} - E_{v1}$) between the first pair of DOS singularities in the valence and conduction bands, as calculated by Charlier and Lambin[14] and by Saito.[15]

The resonant enhancement of the Raman modes in SWNT's was examined theoretically by Richter and

Subbaswamy,[13] who showed that enhancement occurs each time the incident or scattered photon is in resonance with an allowed optical transition $v_j \rightarrow c_i$ from singularity j in the valence band density of states to singularity i in the conduction band density of states. Therefore, the Raman spectrum of the semiconducting SWNT's can be easily enhanced using different laser energies in the range 1–3 eV, since several $v_j \rightarrow c_i$ transitions can occur in this energy range. On the other hand, the resonant enhancement of the Raman cross section for the metallic SWNT's is more selective, and should occur for the nanotube diameters contained in our sample only for the $v_1 \rightarrow c_1$ transition, which corresponds, in the present case, to energies close to 1.9 eV. According to Richter and Subbaswamy,[13] the resonant Raman enhancement for the armchair nanotubes due to the $v_1 \rightarrow c_2$ or $v_2 \rightarrow c_1$ transitions is much smaller than that for the $v_1 \rightarrow c_1$ or $v_2 \rightarrow c_2$ transitions. To interpret our experimental results, we also assume that the Raman intensity for a given vibrational mode under resonance conditions is much greater than off-resonance.

Therefore, a tentative explanation for the difference between the Raman spectrum obtained with $E_{\text{laser}} = 1.92$ eV (and also the $E_{\text{laser}} = 1.96$ eV spectrum) from the spectra using lasers of different energies (see Fig. 3) is that the peaks that appear in all the Raman spectra are mostly associated with resonant Raman effects in the semiconducting SWNT's, whereas the new Raman peaks present in the 1.92 eV laser excitation spectrum are mostly ascribed to the metallic SWNT's. In the $E_{\text{laser}} = 1.92$ eV Raman spectrum, the dot-dashed contribution (see Fig. 5) may be tentatively attributed to semiconducting nanotubes. The downshift of 7 cm^{-1} in the frequencies of the phonons associated with the metallic SWNT's discussed in Sec. IV may be attributed to a coupling between the conduction electrons and the phonons. The large linewidths associated with lines #1 and 3 are attributed to the tube diameter dependence of these mode frequencies, consistent with Fig. 2. The reason why lines #1 and 3 have such large intensities for the metallic nanotubes is not understood and remains an open question.

VI. CONCLUSION

In this work we presented a detailed analysis of the Raman bands associated with tangential C–C stretching modes in the range of 1500–1600 cm^{-1} and the radial breathing mode (RBM) near 180 cm^{-1} of a sample containing single-wall carbon nanotubes (SWNT) with diameters between 1.0 and 1.6 nm using different laser lines between 0.94 eV and 3.05 eV. The RBM bands are quite broad and each one is clearly composed of several different individual peaks with a FWHM linewidth of $\sim$8 cm^{-1}, whose relative intensities are strongly dependent on the photon energy of the exciting laser and on the relative populations of the various nanotube diameters. The resonant behavior of the high frequency band in the range 1500–1600 cm^{-1} is quite different from that for the low frequency band near 180 cm^{-1}. The Raman spectra for the high frequency band obtained with six laser excitation energies in the ranges 0.94–1.59 eV and 2.41–3.05 eV are quite similar, in agreement with the theoretical predictions concerning the weak diameter dependence of the tangential C–C stretching modes. However, the high frequency spectra collected with exciting laser energies close to 1.9 eV are completely different, and reveal an enhancement of the cross section of new Raman modes, not present in the spectra for the other laser lines.

The experimental results are tentatively interpreted in terms of the difference of the electronic density of states (DOS) for the semiconducting and metallic carbon nanotubes. The DOS for the semiconducting nanotubes exhibits several singularities close to the Fermi level, and, in principle, several different electronic transitions in the energy range 0.94–3.05 eV can occur for a semiconducting nanotube with a given diameter. Moreover, the separation in energy for a given electronic transition decreases with increasing diameter. Therefore, in a sample containing a distribution of semiconducting nanotubes with different diameters in the 1.0 to 1.6 nm range, there is a high probability for each incident photon energy to be in resonance with allowed optical transitions for several different semiconducting nanotubes, thus enhancing the cross section of their Raman peaks. On the other hand, the DOS for a metallic nanotube exhibits only a few singularities close to the Fermi level. Recent scanning tunneling spectroscopy (STS) experiments[16] show that the lowest energy separations between singularities in the valence and conduction bands for metallic SWNT's are between 1.7 and 2.0 eV, for nanotubes prepared by the same basic technique.[8] Therefore, the resonant enhancement of the Raman peaks is much more selective in the case of metallic nanotubes, and should occur only for laser energies in approximately the same energy range for the nanotube diameters contained in our samples. According to this interpretation, the new Raman bands observed at 1515 cm^{-1}, 1540 cm^{-1}, 1558 cm^{-1} and 1581 cm^{-1} using the 1.92 and 1.96 eV laser excitation energy are mostly associated with the metallic carbon nanotubes, whereas the other peaks in this spectrum and for the spectra at other laser energies may be attributed to semiconducting nanotubes. The large linewidth of the new Raman lines at 1515 cm^{-1} and 1540 cm^{-1} is attributed to the dependence of these modes on nanotube diameter. The $\sim$7 cm^{-1} downshift of the new modes relative to modes found at other laser energies (and associated with semiconducting nanotubes) is attributed to a coupling between the conduction electrons

and the phonons in the metallic nanotubes that give rise to a mode softening.

Finally, it should be mentioned that experiments on SWNT samples with a smaller diameter distribution or measurements on an individual SWNT will allow the verification of the above interpretation concerning the difference in the Raman spectra of metallic and semiconducting nanotubes, as well as the association of each RBM peak with a particular (n, m) carbon nanotube.

ACKNOWLEDGMENTS

One of us (M.A.P.) is thankful to the Brazilian agency CAPES for financial support during his visit to MIT, and A.M. gratefully acknowledges support from a NATO-CNR fellowship. The Raman measurements in the exciting energy range 1.92–3.05 eV have been performed in the George R. Harrison Spectroscopy Laboratory at MIT supported by the NIH Grant P41-RR02594 and NSF Grant CHE 97-08265. The authors would like to acknowledge Dr. E. B. Hanlon for technical assistance. The measurements with the laser lines 0.94 and 1.17 eV were performed by Dr. B. Chase from the Dupont Experimental Station, Wilmington, DE, USA. The MIT authors gratefully acknowledge valuable discussions with Professor R. Saito of the Electrocommunications University in Tokyo and Dr. J-C. Charlier of the Catholique Universite de Louvain at Louvain-la-Neuve, Belgium, and support for this work under NSF Grant 95-10093 DMR. The UK authors acknowledge support from CAER, NSF Grant OSR-94-52895, and the Department of Energy Contract DE-F22-90PC90029.

REFERENCES

1. S. Iijima, Nature (London) **354**, 56 (1991).
2. R. Saito, M. S. Dresselhaus, and G. Dresselhaus, *Physical Properties of Carbon Nanotubes* (Imperial College Press, London, 1998, in press).
3. R. Saito, T. Takeya, T. Kimura, G. Dresselhaus, and M. S. Dresselhaus, Phys. Rev. B **57**, 4145–4153 (1998).
4. M. S. Dresselhaus, G. Dresselhaus, P. C. Eklund, and R. Saito, Physics World **11** (1), 33–38 (January 1998).
5. M. S. Dresselhaus, G. Dresselhaus, and P. C. Eklund, In *Science of Fullerenes and Carbon Nanotubes* (Academic Press, Inc., New York, 1996).
6. R. Saito, G. Dresselhaus, and M. S. Dresselhaus, J. Appl. Phys. **73**, 494 (1993).
7. M. S. Dresselhaus, G. Dresselhaus, M. A. Pimenta, and P. C. Eklund, *Analytical Applications of Raman Spectroscopy* (Chapman & Hall, London, 1998).
8. A. Thess, R. Lee, P. Nikolaev, H. Dai, P. Petit, J. Robert, C. Xu, Y. H. Lee, S. G. Kim, A. G. Rinzler, D. T. Colbert, G. E. Scuseria, D. Tománek, J. E. Fischer, and R. E. Smalley, Science **273**, 483–487 (1996).
9. S. Bandow, A. M. Rao, K. A. Williams, A. Thess, R. E. Smalley, and P. C. Eklund, J. Phys. Chem. B **101**, 8839 (1997).
10. M. Cardona, in *Light Scattering in Solids II*, chapter: Resonance Phenomena (Springer, Berlin, 1982).
11. A. M. Rao, E. Richter, S. Bandow, B. Chase, P. C. Eklund, K. W. Williams, M. Menon, K. R. Subbaswamy, A. Thess, R. E. Smalley, G. Dresselhaus, and M. S. Dresselhaus, Science **275**, 187–191 (1997).
12. S. Bandow, S. Asaka, Y. Saito, A. M. Rao, L. Grigorian, E. Richter, and P. C. Eklund, Phys. Rev. Lett. **80**, 3779 (1998).
13. E. Richter and K. R. Subbaswamy, Phys. Rev. Lett. **79**, 2738 (1997).
14. J. C. Charlier and Ph. Lambin, Phys. Rev. B (1998, in press).
15. R. Saito (1998, private communication).
16. J. W. G. Wildöer, L. C. Venema, A. G. Rinzler, R. E. Smalley, and C. Dekker, Nature (London) **391**, 59–62 (1998).